Coupled Hydro-Mechanical Analysis of Excavation Damage Zones around an Underground Opening in Sedimentary Rock

H. Abdi[1], T.S. Nguyen[2, 1], E. Evgin[*1], M. Fall[1], and G. Su[2]

[1]Department of Civil Engineering, University of Ottawa, Ontario, Canada
[2]Canadian Nuclear Safety Commission, Ottawa, Ontario, Canada

*Corresponding author: Department of Civil Engineering, University of Ottawa, Ontario, Canada, K1N6N5
eevgin@uottawa.ca

Abstract: Many countries are planning to dispose radioactive waste in deep geologic repositories. An excavation for a repository can cause mechanical damage that affects the fluid flow characteristics of the bedrock. The main objective of the present study is to numerically investigate the extent of the excavation damage zone around an underground opening. The COMSOL Multiphysics code is used to carry out the analysis of a repository under consideration. A relation between the changes in the permeability and the equivalent deviatoric strain is used in the coupled hydro-mechanical analysis.

Keywords: Excavation damaged zone, coupled hydro-mechanical analysis, pore-water pressure.

1. Introduction

The viability of using Deep Geologic Repositories (DGR) for disposing nuclear waste has been investigated in many countries around the world [1, 2]. Underground Research Laboratories (URL) such as those at Mont Terri in Switzerland, Bure in France, and URL in Canada have been built to study the thermal, hydraulic, mechanical and chemical effects of the long term isolation of nuclear waste in rock formations.

It is well known that an Excavation Damage Zone (EDZ) can develop in the vicinity of an underground opening as a result of its excavation [3]. The size of the EDZ and the degree of damage depend on many factors including the in-situ stresses, the excavation technique, the quality of the geologic formation, and the shape of the opening. In addition to the mechanical damage that has the potential to affect the structural stability of an underground opening, the excavation can also affect the fluid flow characteristics of the geologic formation [4]. It is important to note that all physical and chemical processes involved in the radioactive waste disposal are coupled and time dependent processes.

Ontario Power Generation (OPG) [5] is planning to develop a DGR in southern Ontario to host low-level and intermediate-level (LILW) nuclear waste. If approved, the proposed DGR is to be constructed at a depth of about 683 m within an argillaceous limestone. Shafts, tunnels, and a large number of underground emplacement rooms of rectangular shape are to be excavated.

In this paper, a coupled hydro-mechanical analysis is performed to evaluate the short and long term stability of an isolated rectangular emplacement room. The Hoek-Brown parameters are used to obtain the friction angle and cohesion for various types of rocks. An expression relating the changes in the permeability of the rock mass to the equivalent deviatoric strain is used in the hydro-mechanical analysis. The objectives of the present work are as follows: (1) to determine the effect of excavation on stress and strain distributions, (2) to evaluate the effect of time on the short and long term pore pressure response, and (3) to assess the effect of rock damage on hydraulic processes around an emplacement room.

1.1 Geology at the DGR site

Rock formations at the site of the proposed DGR include layers of argillaceous limestone, shale, evaporate and sandstone. The proposed repository is to be located at an approximate depth of 683 m in the Cobourg limestone with high-strength and low permeability (lower than 10^{-21} m^2). Based on the available regional data, it is assumed that the maximum in-situ horizontal stress at the level of the excavation is around 2 times the in-situ vertical stress. The minimum in-

situ horizontal stress is nearly 1.2 times the in-situ vertical stress. In the analysis, it is conservatively assumed that the maximum in-situ horizontal stress is acting perpendicular to the axes of the emplacement room and the direction of the minimum in-situ horizontal stress is parallel to the axes of the emplacement room. The permeability in the horizontal direction at the location of the repository is assumed to be ten times higher than the permeability in the vertical direction.

In this numerical analysis, only four rock layers that surround the emplacement room are included in the analysis. Figure 1 describes the model geometry. These four layers (from the bottom-up) are: a 30 m thick Sherman Fall (SF) layer (layer 1), a 10 m thick Weak Sherman Fall (WSF) layer (layer 2), a 33 m thick Cobourg (C) layer (layer 3), and a 30 m thick Shale (S) layer (layer 4). The emplacement room, which is indicated as EMR in Fig. 1, is of a rectangular shape (8.6 m width x 7 m height), and it is located in the Cobourg formation. The dimensions of the analysis domain are 100 m along the x-axis (horizontal) and 103 m along the y-axis (vertical).

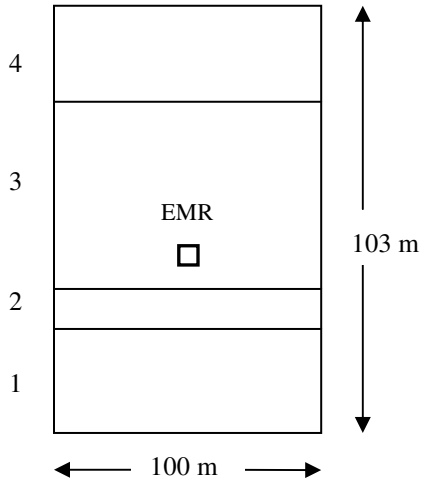

Figure 1. Rock layers and an isolated emplacement room EMR.

1.2 Hydraulic conductivities and pore pressure distribution

The preliminary results of in-situ measurements of the hydraulic conductivity and pore pressure [6] are shown in Figure 2. Preliminary pore pressure measurements were 5.06 MPa and 6.5 MPa at the top and bottom boundaries in Figure 1, respectively. For simplification, it is assumed in this paper, that the pore pressure distribution as a function of depth is linear. The measured values of hydraulic conductivity varied between 10^{-14} m/s and 10^{-13} m/s in the rock units at the proposed repository location.

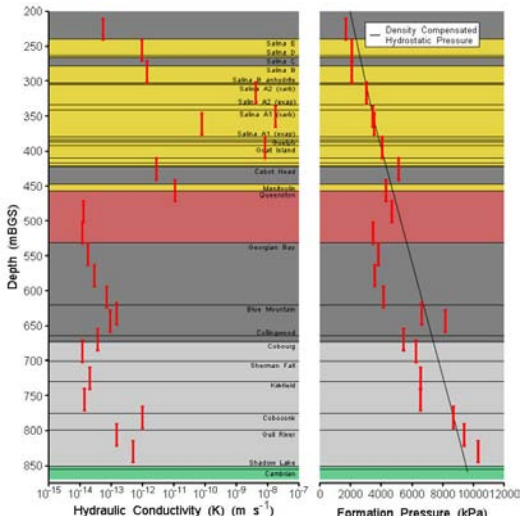

Figure 2. Rock layers, hydraulic conductivities and pore pressures determined by field investigations [6].

2. Finite Element Model

The two dimensional stability analysis of an isolated emplacement room is carried out using the COMSOL Multiphysics code, version 3.5.

2.1 Constitutive relations and parameters

Geotechnical properties of the rock layers are obtained from [5]. The friction angles and the cohesions are calculated from the Hoek-Brown parameters.

Table 1.Geotechnical data used in FE analysis.

Rock Type	E (GPa)	ν	UCS (MPa)	C (MPa)	Φ deg
SF	26.45	0.23	59.88	4.02	36.5
WSF	10.74	0.08	35.76	2.3	34.89
C	36.04	0.19	109.74	9.32	41.34
S	7.3	0.09	31.17	2.04	31.73

E: Young's modulus; ν: Poisson's ratio; UCS: uniaxial compressive strength; C: cohesion; ϕ: friction angle.

Subsequently, the parameters are given as input for the Drucker-Prager elasto-plastic constitutive relation. Table 1 summarizes the data used for the four layers.

2.2 Governing equations

Conservation of Mass:

$$\left[C_s(1-\theta)+C_f\theta\right]\frac{\partial p}{\partial t}+\nabla\cdot\left[-\left(\frac{K_s}{\mu}\right)\left(\nabla p+\rho_f g\,\nabla D\right)\right]=-\alpha_b\frac{\partial \varepsilon_{vol}}{\partial t} \quad (1)$$

Conservation of Momentum:

$$\nabla\cdot\boldsymbol{\sigma}+\alpha_b\nabla p+\boldsymbol{F}=0 \quad (2)$$

where,
C_s & C_f = compressibility of solid and fluid; θ= porosity; K_s= permeability; μ= viscosity; ρ_f = density of the fluid; g= acceleration of gravity; ∇D= unit vector in the direction of g; p= fluid pressure; **σ**= stress tensor; **F**= Body force vector; α_b= Biot-Willis coefficient (It is assumed to be 0.8 for the limestone; ε_{vol}= volumetric strain.

The boundary conditions are as follows. Only vertical movements are allowed at the vertical boundaries of the analysis domain. The top boundary is subjected to a uniform vertical effective stress equivalent to the in-situ vertical effective stress (13 MPa), while the vertical boundaries are subjected to uniform horizontal effective stresses equivalent to the maximum in-situ stress (30 MPa). The base of the model is fixed. Plane strain conditions are imposed. The room is maintained at atmospheric pressure, while the other boundaries are maintained at constant pressures equal to the initial pressures prior to excavation.

3. Results of Analysis

In this section, the data related to the stress and strain distributions, displacements, and pore pressure evolution are discussed. The sign convention adopted is as follows: the compressive normal stress plotted in the figures is negative and the tensile stress is positive.

3.1 Stress distribution

Figure 3 shows the distribution of the vertical compressive effective stress after 2 years from the excavation. Contour lines of the compressive effective stress with a magnitude less than 2e7 Pa are not plotted to maintain clarity. The magnitude of the maximum vertical compressive effective stress in the whole analysis domain is 5.1e7 Pa and it occurred at the corners of the emplacement room.

Figure 4 shows the distribution of the horizontal compressive effective stress after two years from the excavation. The magnitude of the maximum horizontal compressive effective stress is 8.6e7 Pa and it occurs at the corners of the emplacement room. The results indicate that the corners of the room and the areas above and below the room are subjected to high compressive stresses.

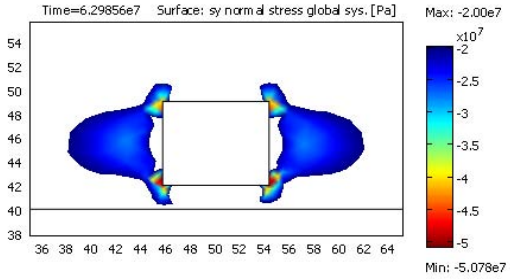

Figure 3. Distribution of σ_y' after two years from the excavation (<-2e7 Pa).

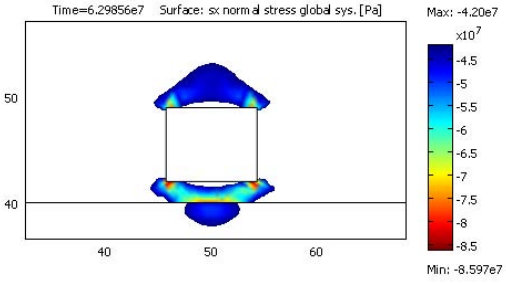

Figure 4. Distribution of σ_H' after two years from the excavation (<-4.2e7 Pa).

3.2 Effective plastic strain distribution

The effective plastic strains caused by the excavation are shown in Figure 5 (ε_p> 0.0001). Largest plastic strains are developed at the corners of the room. Plastic strains also

developed at locations above and below the room and within the weak Sherman Fall layer. The calculated maximum value of effective plastic strain at the corners is about 0.0095.

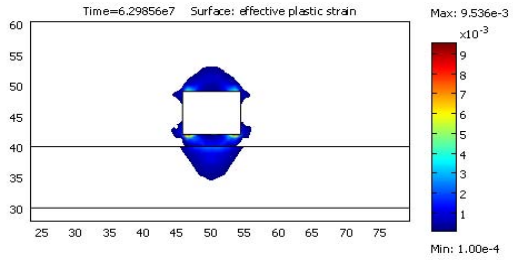

Figure 5. Distribution of the effective plastic strain (>0.0001).

3.3 Volumetric strain distribution

Figure 6 shows the distribution of the volumetric strain at time of 2 years. Expansive volumetric strains are developed on both sides of the room, above and below the room, and within the weak Sherman Fall layer. Compressive volumetric strains are developed at the corners of the room. The expansion of the material can cause an increase in the hydraulic conductivity of the material.

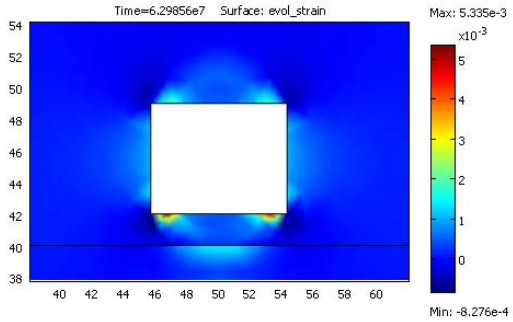

Figure 6. Distribution of the volumetric strain

3.4 Displacements

Table 2 describes the variation of the displacements with time at the crown, the invert, and the spring lines (Spr.). At the spring lines, a maximum inward horizontal displacement of about 8.3 mm is calculated at the end of the excavation. It seems that this displacement is not affected much by time and it remains at a value of 8.5 mm after 10 years. The maximum vertical displacement is 4.3 mm at the crown and 9.3 mm at the invert at the end of the excavation.

Table 2. Displacements versus time at the crown, invert, and spring lines.

Time	Crown (mm)	Invert (mm)	Spr_line (mm)
15 days	4.3	9.3	8.3
2 months	4.3	9.3	8.3
1 years	4.5	9.8	8.4
2 years	4.6	10	8.4
5 years	5	10.6	8.5
10 years	5.4	11.2	8.5

Table 3. Variation of strains with time.

Time	EPS Corner (10^{-3})	EPS Invert (10^{-3})	VS Corner (10^{-3})	VS Invert (10^{-3})
15 d	3.8	0.28	0.45	0.6
2 mon	4.3	0.27	0.8	0.6
1 y	5.7	0.29	1.56	0.59
2 yrs	6.2	0.24	2.1	0.58
5 yrs	7.1	0.14	2.65	0.59
10 yrs	7.5	0.1	3.1	0.57

These displacements increased with time and reached values of about 5.4 mm and 11.2 mm for the crown and the invert after ten years. The results indicate that the EDZ is not uniform around the room and the displacements can increase with time at some locations within the EDZ.

3.5 Variation of strains with time

Table 3 describes the variation of the effective plastic strain (EPS) and the volumetric strain (VS) with time at the bottom left corner and the invert of the emplacement room. After ten years from the excavation, the effective plastic strain at the corner almost doubled while the volumetric strain increased five times. At the invert, no significant increase is calculated for both effective plastic strain and volumetric strain. This indicates that the degree of change in strains with time is not the same in all locations within the EDZ.

3.6 Pore pressure generation and dissipation

At the end of the excavation the pore pressure at the boundaries of the room reduces to the

atmospheric pressure and the room acts as a sink. The shape of the excavation has an effect on the response of the rock mass to an excavation.

The damage to the rock affects the flow characteristics of the material. In the present analysis, two cases of permeability are considered. In the first case, the permeability is kept constant which means the effect of the mechanical damage on permeability is neglected. In the second case, the effect of damage on permeability is considered by expressing the permeability as a function of the equivalent deviatoric strain.

3.6.1 Case 1: Constant permeability

The pore pressure (PP) at the level of the emplacement room before the excavation was around 5.9e6 Pa. For clarity, in the following figures only the pore pressures greater than 5.9e6 Pa (PPG) are plotted. Figure 7 shows the PPG generated at the end of the excavation. High PPGs are developed in the highly compressed areas. The maximum pore pressure is around 2.3e7 Pa and it is developed at the corners of the emplacement room. Most of the PPG is dissipated after two years from the excavation as can be seen in Figure 8.

As soon as the excavation begins, the pore pressure starts to change and redistribute in the surrounding areas. Figure 9 shows PP distribution two months after the excavation.

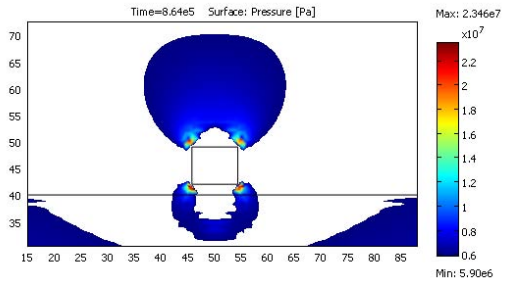

Figure 7. Pore pressures >5.9e6 Pa (PPG) at the end of the excavation.

The pore pressure is negative in the areas up to a distance of 4 m away from the vertical sides of the opening, and also on the roof and the floor (2~3 m) due to volumetric expansion.

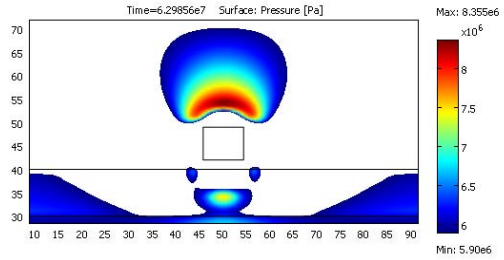

Figure 8. Pore pressures >5.9e6 Pa (PPG) two years after excavation.

The excess pore pressure is also negative above and below the room. The redistribution of pore pressure evolves with time.

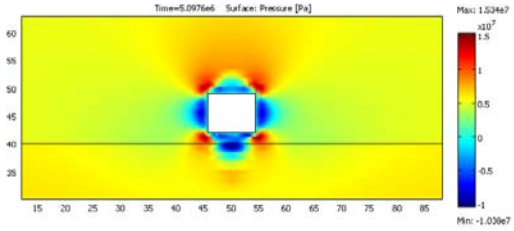

Figure 9. Pore pressure (PP) distribution after two months from the end of excavation.

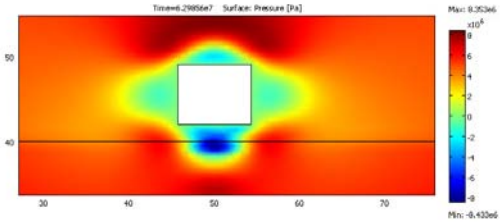

Figure 10. Pore pressure (PP) distribution after two years from the excavation.

Figure 10 shows its distribution after two years from the excavation. The anisotropy in permeability, the low permeability values, and the high stresses generated by the excavation are affecting the patterns of pore pressure distribution. Due to the low permeability of the rock, it could be seen that the pore pressure has not reached a steady state after two years.

3.6.2 Case 2: Permeability as a function of equivalent deviatoric strain

Excavation induces damage in rock. As a result, the material may expand in some areas around the opening and, consequently, the permeability

may increase. In order to simulate the increase in permeability, we used Eq. 3 [2].

$$k = k_{ini}\, e^{7000\, \varepsilon_d} \quad (3)$$

$$\varepsilon_d = \frac{\sqrt{2}}{3}\left((\varepsilon_{11}-\varepsilon_{22})^2 + (\varepsilon_{22}-\varepsilon_{33})^2 + (\varepsilon_{11}-\varepsilon_{33})^2 + 6\,\varepsilon_{12}^2 + 6\,\varepsilon_{13}^2 + 6\,\varepsilon_{23}^2\right)^{1/2} \quad (4)$$

where: ε_d is the equivalent deviatoric strain and k_{ini} is the permeability of the undamaged rock.

In order to avoid numerical convergence problems, the value of the permeability is not allowed to increase more than 10^3 times the initial value. Figure 11 describes the PPG generated at the end of the excavation. After the excavation, the pore pressure continues to evolve with time. Figure 12 gives the PPG distribution two years after the excavation. A comparison of Figures 8 and 12 indicates that the increase in permeability due to damage speeds up the pore pressure dissipation.

Figure 13 shows the PP distribution two months after the excavation. Figure 14 shows the PP distribution two years after the excavation.

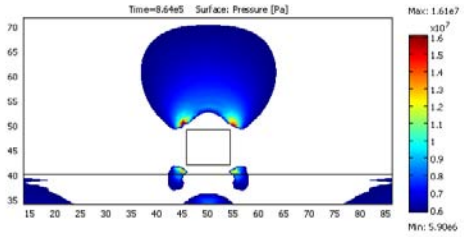

Figure 11. Pore pressures >5.9e6 Pa (PPG) at the end of excavation for variable permeability.

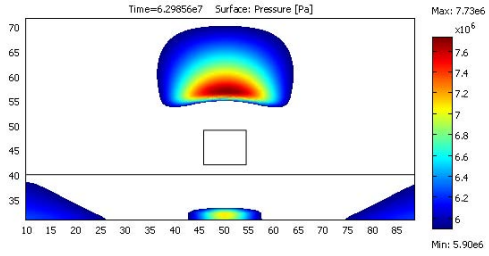

Figure 12. Pore pressures >5.9e6 Pa (PPG) two years after excavation for variable permeability.

3.6.3 Pore pressures in compressed and expanded areas

The four points shown in Figure 15 are used to investigate the effect of compression or extension on the dissipation of pore pressure with time. Points 1 and 3 are located at a distance of 1.5 m away from the excavation. Points 2 and 4 are 4 m away from the excavation. Points 1 and 2 are located in a compressed area, whereas, points 3 and 4 are located in an expanded area. Two cases of permeability are considered: (a) constant and (b) variable.

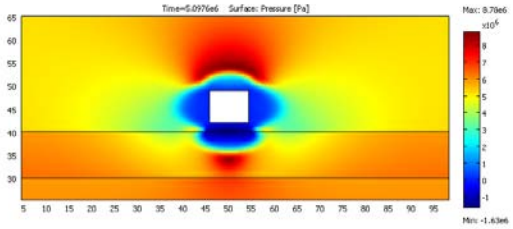

Figure 13. Pore pressure (PP) distribution two months after the excavation, for variable permeability.

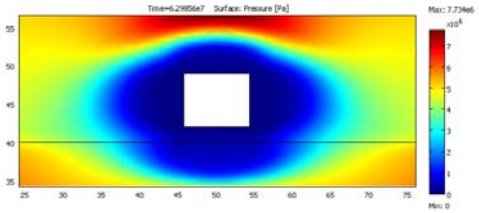

Figure 14. Pore pressure (PP)distribution after two years from the excavation, for variable permeability.

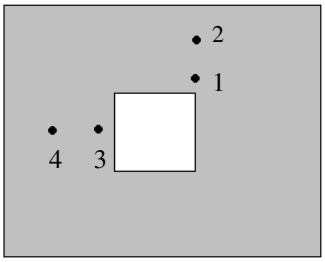

Figure 15. Selected points from the domain to track the pore pressure variation with time.

For the case of constant permeability, the generation and dissipation of pore pressure with time at the selected points are shown in Figure 16. In the compressed areas, the pore pressure reaches a maximum value at the end of the excavation. After some time, PP starts to dissipate and it takes years to completely dissipate. The pore pressure is higher in the vicinity of the opening than in the areas located

far away from the opening. But, PP tends to dissipate more quickly in the areas near the opening. In the expanded areas, the pore pressure starts to dissipate as soon as the excavation starts and reaches the atmospheric pressure in months. The negative pressure developed at point 3 is due to the expansion of the material.

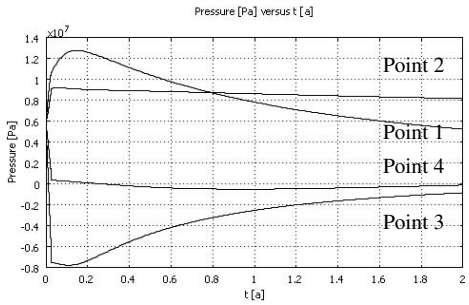

Figure 16. Variation of pore pressure with time (years) at selected points (constant permeability).

For variable permeability, the variation of the pore pressure with time at the selected points is shown in Figure 17. In general, similar behavior is observed as in the previous case of constant permeability. But here, in compressed areas, the pore pressure dissipates more quickly. In expanded areas, the pore pressure tends to reach the atmospheric pressure in days after the excavation.

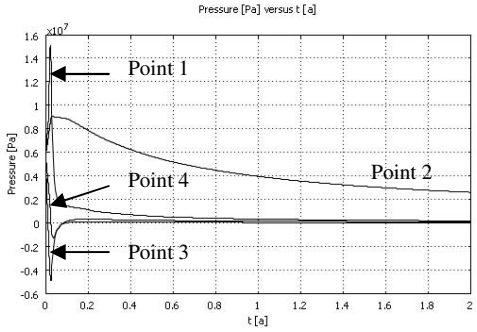

Figure 17. Variation of pore pressure with time (years) at selected points (variable permeability).

7. Conclusions

The conclusions of the hydro-mechanical coupling analysis are summarized below.

1. An excavation causes stress concentrations at the corners of a rectangular shape repository.
2. Large volumetric strains and effective plastic strains develop around the room and in the weak Sherman Fall layer. These strains increase with time.
3. The EDZ is not uniformly distributed around the emplacement room. The size of the EDZ changes with time.
4. The degree of the damage within the EDZ is not the same in all locations.
5. The pore water pressure dissipation is faster in the analysis with variable permeability than the analysis with constant permeability.
6. The type of volumetric strain (expansion or compression), the stress concentrations generated by the excavation, the low permeability of the material, and the anisotropy in permeability have a significant role in the development and dissipation of the pore pressure.

8. References

1. Rutqvist J, Borgesson, L., Chijimatsu, M., Hernelind, J., Jing, L.,Kobayashi , A. and Nguyen, S. Modeling of damage, permeability changes and pressure responses during excavation of the TSX tunnel in granitic rock at URL, Canada. *Environmental Geology*, **57**: 1263-1274, (2009).

2. Nguyen, T. S. Excavation damage and pore pressure evolutions around a test tunnel in granite, *Proceedings of the Canadian Geotechnical Conference*, Ottawa, (2007).

3. Malmgren, L., Saiang, D., Toyra, J., and Bodare, A. The excavation disturbed zone (EDZ) at Kiirunavaara mine, Sweden—by seismic measurements. *Journal of Applied Geophysics*, **61**(1), (2007).

4. Souley, M., Homand, F., Pepa, S., and Hoxha, D. Damage-induced permeability changes in granite: a case example at the URL in Canada, *International Journal of Rock Mechanics and Mining Sciences*, **38**(2), (2001).

5. OPG Report - 1. Phase 1 Long-Term Cavern Stability, Prepared by ITASCA Consulting Group, Inc., OPG 00216-REP-01300-00005-R00, (2008).

6. Avis J., Lam T., Roberts R., Chace D., Toll N., and Beauheim, R.. Hydraulic testing to characterize low permeability sedimentary formations – proposed Deep Geologic Repository, Tiverton, Ontario. *GeoHalifax*. Halifax, NS, Canada. (2009).